

Velocity mapping of gasflow in the upper airways of a lung model for validation of computational fluid dynamics simulations

Guilhem Jean Collier¹, Jim Wild¹, George Oates², and Yongmann Chung²

¹Department of Cardiovascular Science, The University of Sheffield, Sheffield, Yorkshire, United Kingdom, ²Centre for Scientific Computing, University of Warwick, Coventry, United Kingdom

Target audience: Lung MRI, flow imaging

Purpose: This work presents an MRI alternative to Particle Image Velocimetry (PIV) for validating Computational Fluids Dynamics (CFD) simulations of airflow in a geometry model of the upper airways derived from CT data sets.

Introduction: Non-invasive measurements of airflow distribution in the airways could help in understanding airflow in obstructive lung diseases and in predicting the particle and aerosol deposition process in inhaled therapy research. CFD simulations made on compliant airway models obtained through additive layer manufacturing are used to study airflow but usually need experimental validation with PIV¹. Phase Contrast Velocimetry (PCV) MRI of hyperpolarized (HP) ³He can be used to generate velocity maps in-vitro² and in-vivo³. This work develops experimental MRI techniques for CFD airflow model validation by testing new fluids with different dynamic properties. Constraints to the use of ³He are its cost and its signal losses by free diffusion in MRI gradients. ¹²⁹Xe being a much heavier atom, its free diffusion is smaller however its gyromagnetic ratio is three times lower than for ³He. H₂O has a much higher density, so lower flows are required to match the flow regime of airflow and its Reynolds number (Re). In this work we propose the use of PCV MRI of H₂O as a mimic for flow imaging models of the upper airways.

Materials and Methods: The PCV sequence is a multiple interleaved 2D Cartesian spoiled gradient echo using a 4 point balanced velocity encoding scheme. It was implemented on a GE HDx 1.5T scanner. The airway model is derived from rapid prototype models of CT scans of the upper airways⁴ (from the trachea down to the 4 to 6 generation) at the scale 1.5:1 (Fig. 1). The CFD simulations were performed using the finite-volume CFD code, Star-CCM+. A second-order finite volume method was used with the SIMPLE algorithm for pressure-velocity coupling. The three-dimensional computer model of the lung was constructed, and polyhedral computational grids were generated for the geometry shown in Fig. 1. The trachea inlet section was extended smoothly to a circular pipe, and a parabolic of steady laminar flow was applied as an inlet condition. The constant pressure condition was applied at each outlet. Experimentally, the fluid was administrated to the trachea of the airways model through a pipe of similar diameter and long enough to obtain a fully-developed flow. The model was enclosed hermetically into a container such that a pressure difference could be applied between the input and the outputs of the lung model. In the case of H₂O, the flow was created by a height difference between inlet and outlet. ³He and ¹²⁹Xe were mixed with nitrogen after being polarized on-site with spin exchange polarizers providing polarization values of 25 % and 15 % respectively, and the gas flow was measured by a pneumotachograph. More than 15 different slice locations from the inlet of the trachea to the 3rd airway generation were measured with water for flows varying from 5.6 to 20 mL/s (400 < Re < 1450). Four locations from the trachea to the 1st airway generation were measured with ³He (flow of 130 mL/s, Re = 400) and ¹²⁹Xe (flow of 130 mL/s, Re = 880) corresponding to slow breathing conditions. All data were reconstructed offline using the phase difference reconstruction to extract the 3 velocity components of each pixel. After phase reconstruction, manual phase unwrapping and phase offset correction were implemented when necessary and a binary mask based on signal intensity threshold was multiplied with the obtained velocity maps.

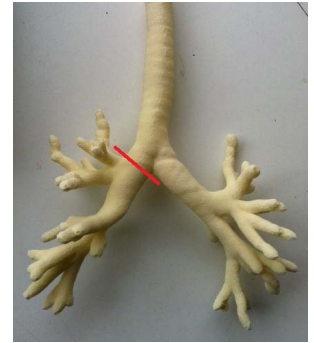


Figure 1: Picture of the lung model used for experiments and CFD simulations.

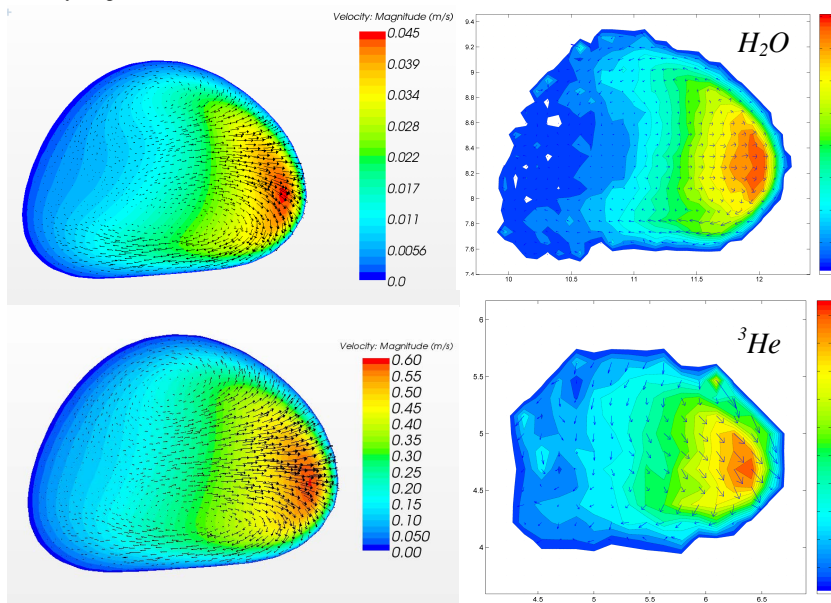


Figure 2: Comparison between CFD simulations (left) and experimental velocity maps (right) measured in the right main bronchus at the slice location of Fig. 1. Top: flow of water (9 mL/s, Re = 465, 3 mm slice thickness, 0.86*0.86 mm² in-plane resolution, 40° flip angle, T_E/T_R = 10.4/200 ms and SNR of 60). Bottom: flow of HP ³He (125 mL/s, Re = 380, 1 cm slice thickness, 1.56*1.56 mm² in-plane resolution, 31° flip angle, T_E/T_R = 5.2/9.5 ms and SNR of 40). The colored contours represent the absolute velocity in m/s for CFD simulation and cm/s for experimental data. The vectors are showing the transverse motion.

Acknowledgements to the European Union FP7 project AirPROM for funding.

Results and discussion: On Fig. 2, a comparison between CFD simulations and MRI results obtained with proton (Re ~ 465) and ³He (Re ~ 380) is shown. As expected due to the lower polarization and γ , the SNR for ¹²⁹Xe was more than 2 times lower than that for ³He. SNR of 40 were obtained with ³He for a resolution of 1.6 mm leaving the possibility to achieve in future experiments the best resolution set by ³He free diffusion (~ 1 mm). A relatively good agreement between HP gas experiments and CFD simulation was found but some phase errors occurred when the slice was not in the centre of the magnet due to the concomitant fields (see vertical component of figure 2.c). The artefact in the phase was more noticeable with H₂O compared to the HP gas but it was easily corrected in the proton experiments by performing the same sequence without flow and subtracting the phase offsets from the first experiment. Moreover, the resolution obtained with proton experiments was higher (0.9 mm) for the same SNR and a very good correlation with CFD simulation is demonstrated (see Fig. 2.a and 2.b). In conclusion, MRI provides experimental measurement of the three velocity components of flow in a realistic model of human proximal airways. Water can be used as an MR sensitive mimic for HP gas in these experiments by careful choice of flow regime to match the Reynolds number of the respective fluid. Further work will focus on developing more realistic models (new compliant model with more airway generations, inlet conditions including pharyngeal airways, semi rigid material taking into account airway resistance), rapid imaging to obtain flow during a breathing cycle, and a more automated way to control and change the flow conditions.

References: 1 K. Adler et al. Experiments in Fluids, vol. 43: 411-423, 2007; 2 L. De Rochefort et al. Journal of Applied Physiology, vol. 102: 2012-2023, 2007; 3 L. De Rochefort et al. Magnetic Resonance in Medicine, vol. 55: 1318-1325, 2006; 4 F. Giesel et al. Academic Radiology, vol. 16: 495-498, 2009.